Solar and Heliospheric Observatory (SOHO) Flight Dynamics Simulations Using MATLAB®*

R. D. Headrick and J. N. Rowe
Computer Sciences Corporation (CSC)
Lanham-Seabrook, Maryland, USA 20706

Abstract

This paper describes a study to verify onboard attitude control laws in the coarse Sun-pointing (CSP) mode by simulation and to develop procedures for operational support for the Solar and Heliospheric Observatory (SOHO) mission. SOHO was launched on December 2, 1995, and the predictions of the simualtion were verified with the flight data. This study used a commercial off-the-shelf (COTS) product (MATLAB®) to do the following:

- Develop procedures for computing the parasitic torques for orbit maneuvers

- Simulate onboard attitude control of roll, pitch, and yaw during orbit maneuvers

- Develop procedures for predicting firing times or both on- and off-modulated thrusters during orbit maneuvers

- Investigate the use of feed-forward or prebias torques to reduce the attitude hangoff during orbit maneuvers—in particular, determine how to use the flight data to improve the feed-forward torque estimates for use on future maneuvers.

The study verified the stability of the attitude control during orbit maneuvers and the proposed use of feed-forward torques to compensate for the attitude hangoff. Comparison of the simulations with flight data showed that

- Parasitic torques provided a good estimate of the on- and off-modulation for attitude control

- Feed-forward torque compensation scheme worked well to reduce attitude hangoff during the orbit maneuvers

The work has been extended to prototype calibration of thrusters from observed firing times and observed reaction wheel speed changes.

This study demonstrated the use of MATLAB® simulations to support flight dynamics analysis and development of operational procedures in the Goddard Space Flight Center (GSFC) Flight Dynamics Division (FDD).

1.0 Introduction

During orbit maneuvers, SOHO attitude control system (ACS) in the CSP mode is subject to disturbance torques from several sources: thruster alignment, hot/cold burning of thrusters, payload movement, fuel slosh, and solar array flexing. Analysis of the control laws by Smallwood (Reference 1) indicated an attitude hangoff because of these disturbance torques, which could be compensated in the control loops by uplinking a feed-forward torque to improve the pointing performance. To meet the Flight Dynamics requirement to provide inflight estimation of the disturbance torques, prelaunch analysis (Reference 2) recommended using the average pointing errors (the difference between the commanded and ground-computed attitude angles) during an orbit maneuver to estimate the feed-forward torque for the next maneuver.

This paper reports work in modeling the propulsion and attitude control systems to verify this procedure through simulation and SOHO flight experience in using it. Thruster and center of mass (CM) alignment effects were also predicted and evaluated from a computer-assisted plant identification technique.

2.0 Simulation

A description of the simulation models in this study and the results are given below.

2.1 Simulation Models

A key feature of the SOHO propulsion system is the coupling of the roll, pitch, and yaw control loops through "parasitic" torques. Parasitic torques, $\vec{T}_{po}$, are unwanted torques generated during thrusting (e.g., a delta-V in the z direction, applying torque about the x-axis), which also affect the other two axes. They occur because the thrusters are not mounted along orthogonal axes. These torques cause attitude-pointing errors to grow in the control loop until they exceed a deadband limit and a thruster fires to compensate.

The simulation was implemented using MATLAB®, a commercial software tool designed for matrix manipulation and control law simulation. The simulation was designed with the following features and limitations:

- The thruster model of $\vec{R} \times \vec{F}$ torques is based on the manufacturer's values of location, direction, nominal CM, and average beginning of life (BOL) thrust magnitude. Provision is made for easily modifying the CM to study the sensitivity to changes that are expected with fuel usage. In addition, the user can modify the direction and efficiency of the thrusters to adjust the model. Orbit thrusters (see Figure 1 on the next page) are fired in couples about the primary axis. The thruster configuration is shown in Table 1.

Table 1. Definition of Cases for Orbit Thrust Simulations

Case No.*	Delta-V Direction	Thruster Pair	Torque Axis
1	−X	1 / 2	Y (pitch)
2	+X	3 / 4	Z (yaw)
3	−Z	5 / 6	X (roll)
4	+Z	7 / 8	X (roll)

* The case number refers to British Aerospace (BAe) simulation cases (Reference 3)

- Pulse-width modulation (PWM) is simulated with the onboard computer (OBC) values for minimum on time and saturation (References 2–5). The on-modulation axis control model is shown in Figure 2 (from Reference 3). The control loop converts torque demand to thruster on time and induces a reactive thrust torque when the on time is above the minimum or deadband. While delta-V thrusting is active, the primary torque axis is off modulated; that is, the thruster firing is nearly continuous during the burn while maintaining the attitude-pointing errors within deadband limits. Off modulation rebalances the thruster torques based on the attitude reaction by reducing the on time of one of the paired thrusters and increasing the on time of the other. On modulation and off modulation can occur simultaneously on different axes.

- To model steady-state behavior, thrust level is approximated as the average during the 2-second actuation period, ignoring details of thruster ramp up and time delays.

- The spacecraft rigid body dynamics model is given by

$$I\dot{\vec{\omega}} = \vec{N}_{th} - \vec{\omega} \times \vec{L}$$

where I = moment of inertia tensor
  ω = body rate vector
  N = thruster torque vector
  L = total angular momentum vector given by

$$\vec{L} = I\vec{\omega} + \vec{h}_{wh}$$
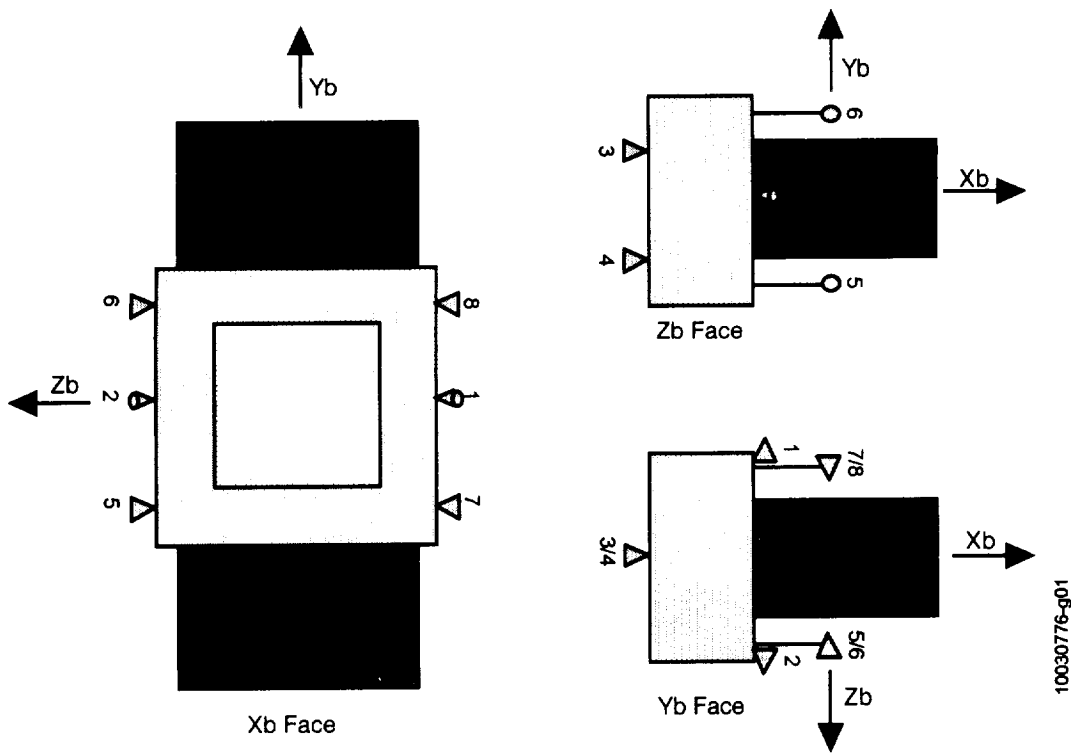
where $\vec{h}_{wh}$ is the wheel angular momentum vector.
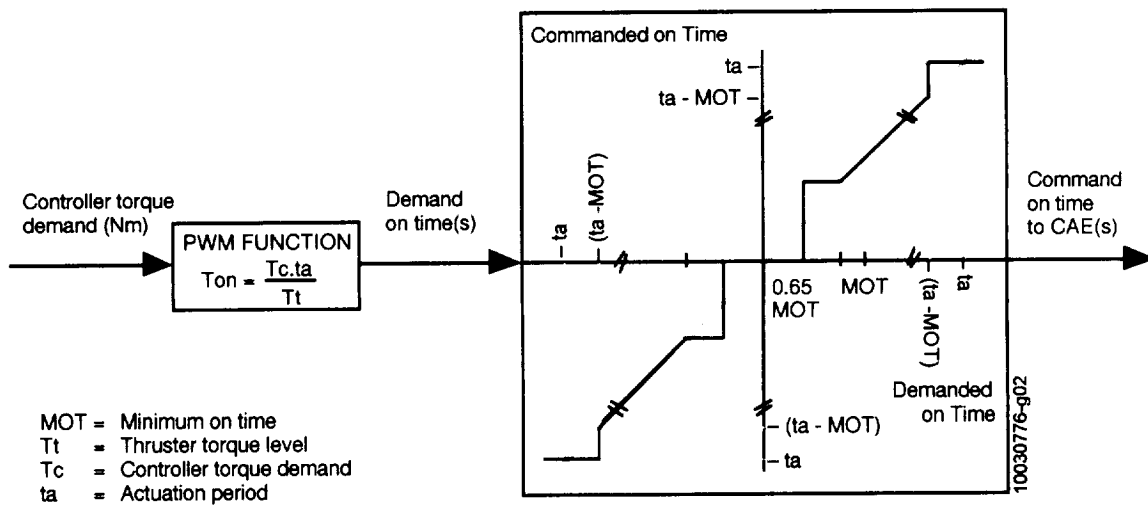
Figure 1. SOHO Spacecraft Thruster Orientations

MOT = Minimum on time
Tt = Thruster torque level
Tc = Controller torque demand
ta = Actuation period

Figure 2. PWM Function of On Modulation

113

Torque from solar radiation pressure ($\sim 10^{-7}$ Nm) is negligible compared to thrust torques. The simulation ignores contributions from fuel sloshing, solar panel flexure, and antenna motion, because they have transient effects. Plume impingement is not modeled.

Figure 3 is a block diagram of the model. The left half of the diagram shows the control section, with provision for input for delta-V and feed-forward torques. The PWM block indicates deadband and saturation for thrust on each axis. Cross-coupling is shown explicitly, where the cross-terms include the parasitic torques and the $\vec{\omega} \times \vec{L}$ term.

The right-hand side of the block diagram shows the second order model that is symmetric for the three loops. They are represented by the discrete time equations

$$\dot{\vec{x}}_{i+1} = \dot{\vec{x}}_i + \dot{\vec{\omega}}_i dt$$

$$\vec{x}_{i+1} = \vec{x}_i + \dot{\vec{x}}_i dt$$

where the state vector $\vec{x}$ consists of the attitude angles $\vec{x} = (\phi \quad \theta \quad \psi)^T$, where ϕ – roll, θ – pitch, ψ – yaw, and $\dot{\vec{x}}$ – the rates. The control vector $\dot{\vec{\omega}}$ is updated at the 2-second actuation period and includes the cross-coupling effects. The time equations are integrated over the OBC cycle of 0.05 second.
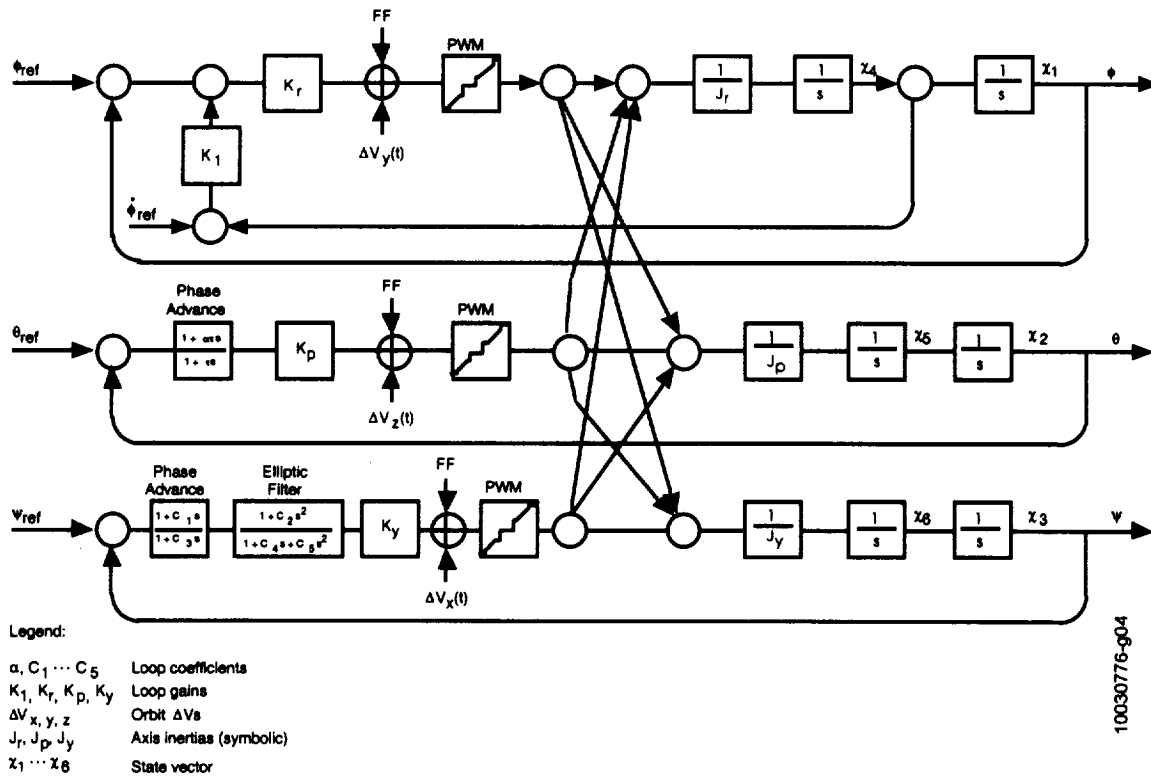

Figure 3. Schematic of Coupled Attitude Control Loops

2.2 Simulation Results

Figures 4 through 6 illustrate the occurrence of pointing errors during delta-V −X thrusting (case 1). The pointing errors arise from two sources: the effects from the parasitic torques and the offsets from a position-only controller. The secondary axes react to parasitic torques with their on-modulated control torques when they exceed the minimum. The simulator reproduced the general patterns of the BAe simulations (Reference 3) cases 1 through 4 for delta-V in ±X and ±Z directions. (BAe's performance analysis demonstrated the stability of the SOHO ACS under worst-case conditions, while our purpose was to define ground support procedures for SOHO Flight Dynamics.) Figure 7(a) shows a single-sided deadband pattern in pitch, and Figure 7(b) shows the pitch pointing error reduction after including a feed-forward torque from the measured pointing error.

The initial estimate of the feed-forward torque, $\vec{F}_0$, was calculated from

$$\vec{F}_0 = -\mu\vec{T}_{po}$$

where μ is the percent on time for the off-modulated axis (nominally 75 percent), and $\vec{T}_{po}$ is the nominal parasitic torque calculated from

$$\vec{T}_{po} = \vec{N}_+ + \vec{N}_-$$

where $\vec{N}_+$ and $\vec{N}_-$ are the torque vectors (based on location, direction, CM, thrust, and efficiency) applied in the positive or negative sense about the control axis. For subsequent maneuvers, the attitude hangoff is evaluated and a new value is calculated for the feed-forward torque, $\vec{F}_{new}$, for uplink on the next maneuver

$$\vec{F}_{new} = \vec{F}_0 - \vec{T}_D$$

where, for each axis,

$$T_{D_i} = K_i \times \Gamma_{meas_i}$$

In these equations, $\vec{\Gamma}$ is the attitude hangoff, $\vec{K}$ is the loop gain, and $\vec{F}_0$ is the value of feed-forward torque at which $\vec{\Gamma}$ was measured.
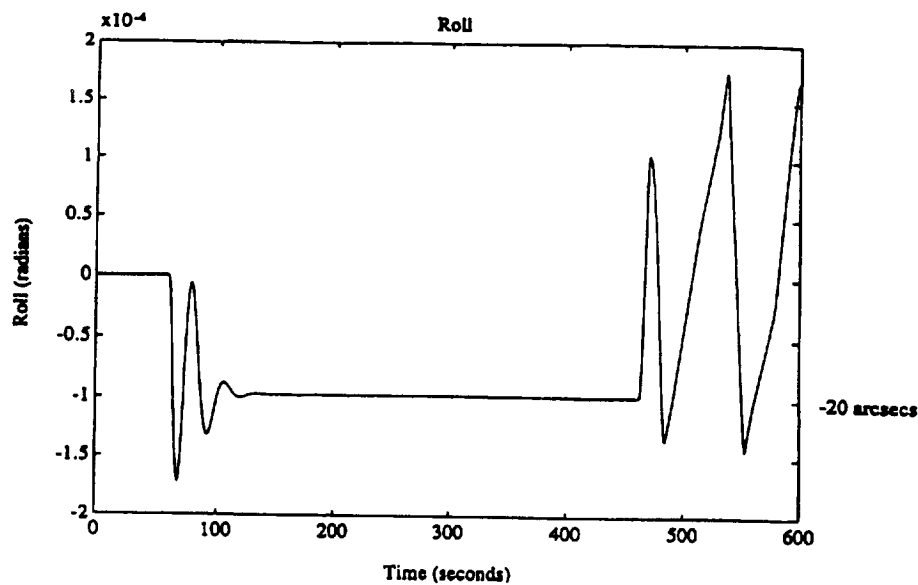

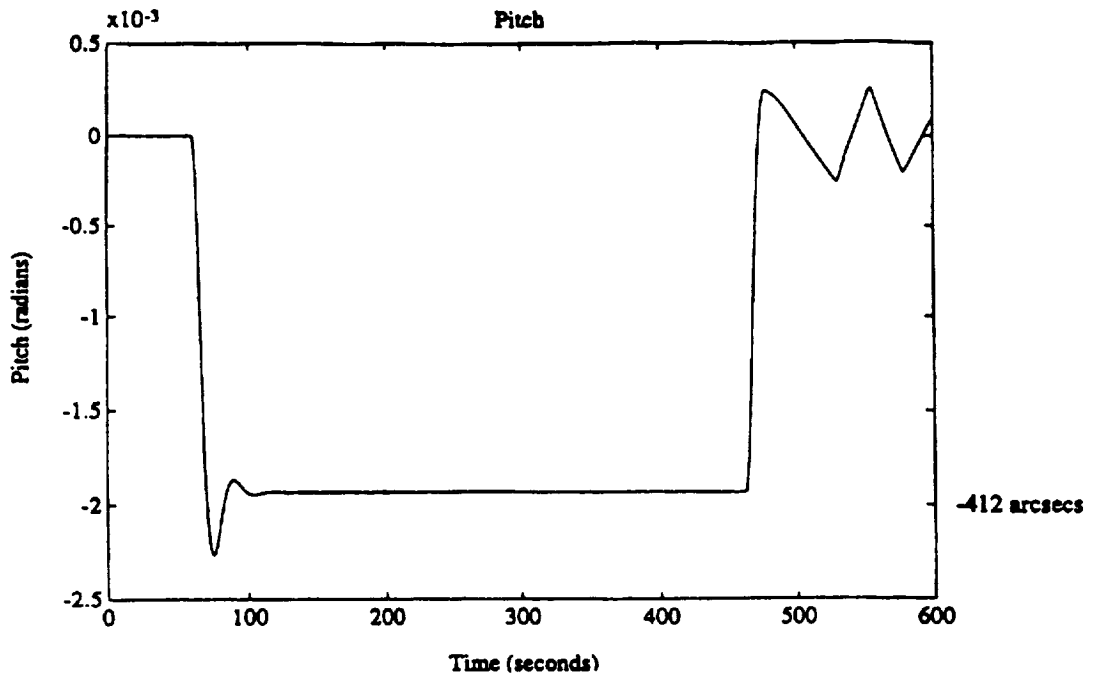**Figure 4. Spacecraft Roll Angle for −X Delta-V (Case 1)**

Figure 5. Spacecraft Pitch Angle for –X Delta-V (Case 1)
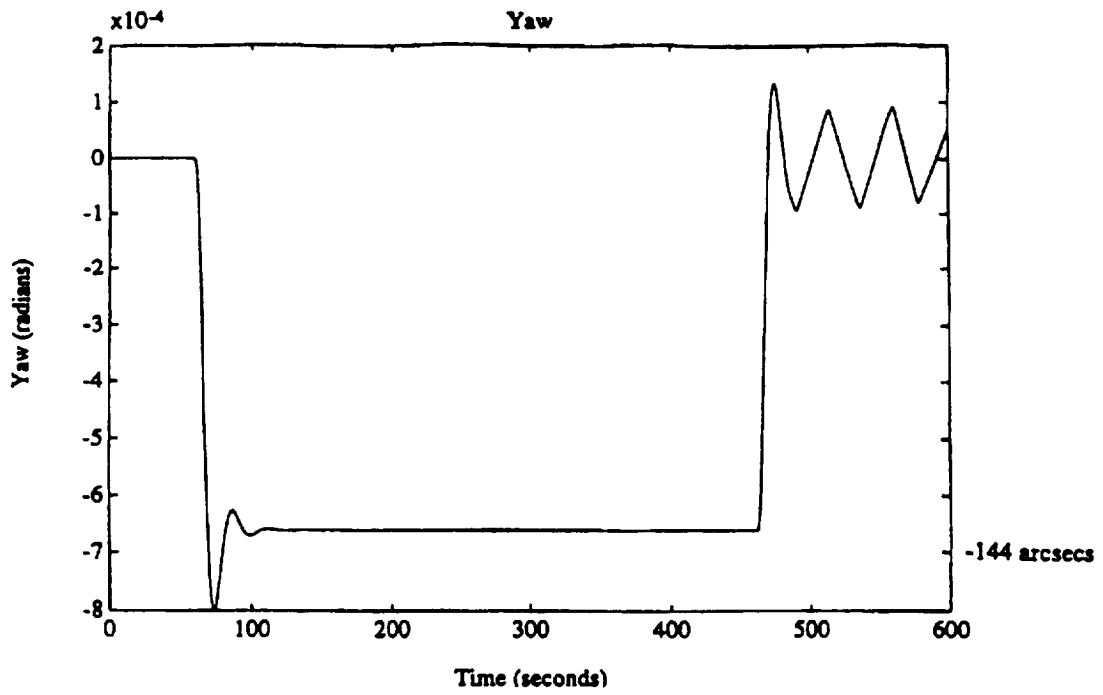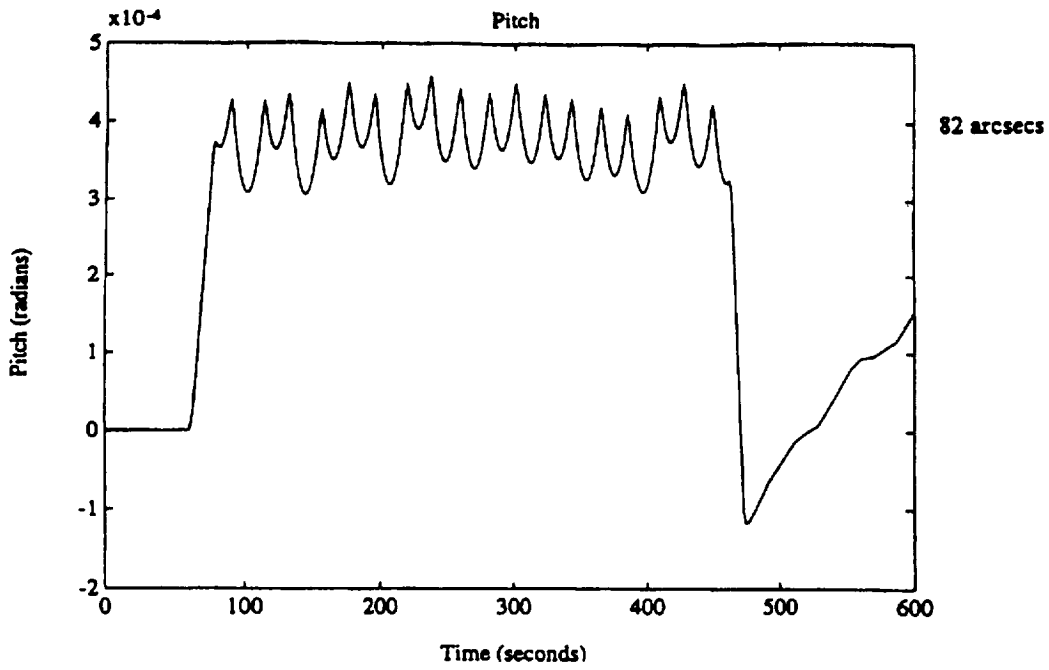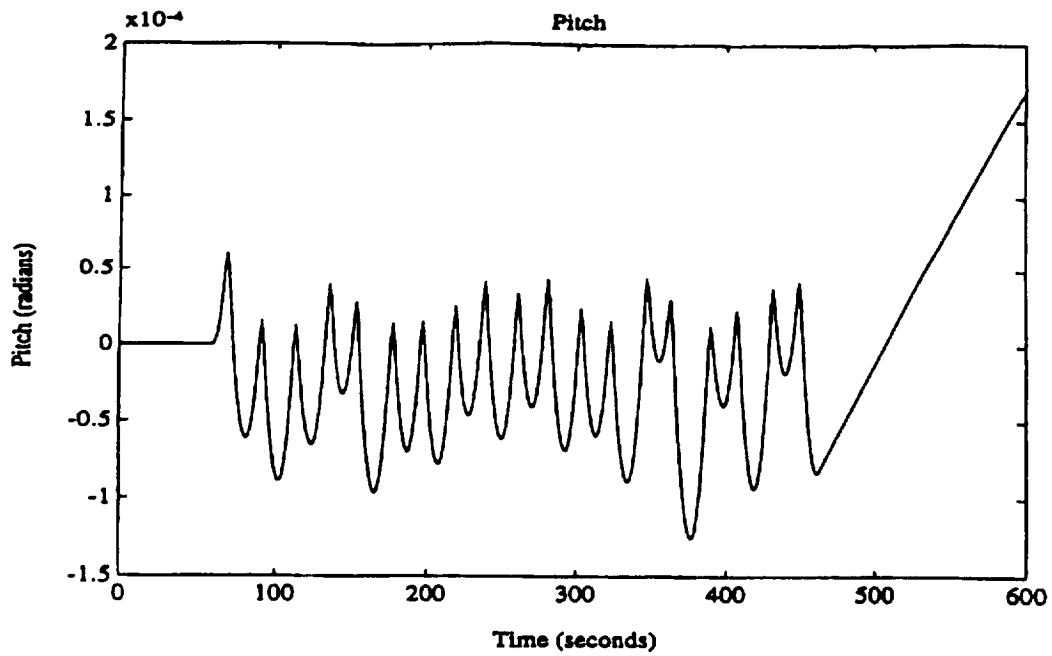

Figure 6. Spacecraft Yaw Angle for –X Delta-V (Case 1)

116

(a) Initial Feed-Forward

(b) Feed-Forward

Figure 7. Spacecraft Pitch Angle for +X Delta-V (Case 2)

117

3.0 Flight Experience

SOHO flight experience involving feed-forward torques and thruster alignment are described in the following sections.

3.1 Feed-Forward Torques

This section discusses the results of the first three orbit maneuvers on SOHO in terms of attitude hangoff and the use of feed-forward torques to compensate.

Table 2 shows a summary of the values observed on SOHO for the roll axis. The hangoffs in pitch and yaw were ≤ 0.03 deg, and no attempt was made to compensate for those. The "thrusters" column in this table indicates which thrusters were used to provide the delta-V.

Table 2. Summary of Roll Axis Feed-Forward Torques

Maneuver	Segment	Thrusters	F_0 (Nm)	Attitude Error Γ (deg)	F_{new} (Nm)
MCC1	X-1	1A, 2A	0	+0.07	−0.096 (a)
	X-2	1A, 2A	0	— (b)	—
MCC2	Z-1	7A, 8A	−0.096	−0.08	+0.10
	Z-2	7A, 8A	+0.10	+0.03	+0.042 (c)
	X-1	1A, 2A	+0.10	+0.13	−0.15
HOI	X-1	1A, 2A	−0.15	+0.04	

Notes: (a) Calculated based on a hangoff of 0.05 to be conservative
(b) Not obtained because of telemetry gap at start of maneuver
(c) Not used because the next maneuver was in the X-direction

These results are based on visual analysis of plots of the roll attitude. As the difference between the commanded and achieved attitudes, hangoff is visible as a jump in angle at the start of a maneuver. The hangoff at the end of the maneuver was more difficult to estimate because of control system settling (and its deadband). Figures 8 and 9 show as examples the transitions at the start and end of the midcourse correction (MCC)2 X-1 maneuver. This may be compared with Figure 10, which shows the start of the halo orbit insertion (HOI) X-1 burn where the hangoff is significantly smaller. The ramp in Figure 10 before the maneuver start is caused by a small residual intertial reference unit (IRU) bias.

Comparing the MCC2 Z-1 and Z-2 burns and the MCC2 X-1 with HOI X-1 shows that the technique of uplinking feed-forward torques does reduce the attitude errors, although because they are already small, it is not necessary for successful execution of the maneuvers.

3.2 Thruster Alignment

Prelaunch and postlaunch thruster analysis and the thruster results are discussed in the following subsections.

3.2.1 Prelaunch Thruster Analysis

The predicted burn times of the secondary thrusters are a byproduct of the ACS simulations. As a result, this study was extended to support prelaunch thruster analysis. In CSP mode, the momentum wheels are free running and the attitude angles are controlled to their commanded values (usually zero). Thus, any torque applied by the primary thruster pair (off modulated) must be compensated by firings of secondary (on-modulated) thrusters. This analysis showed that the secondary burn times can be predicted with good accuracy from the thrust torque vectors alone. This is an important result, because it removes reliance on the accuracy of any simulation. While these firings are a small fraction of the main thrusts, their effects were predictable in advance and were included in delta-V targeting for the highly successful major orbit maneuvers.
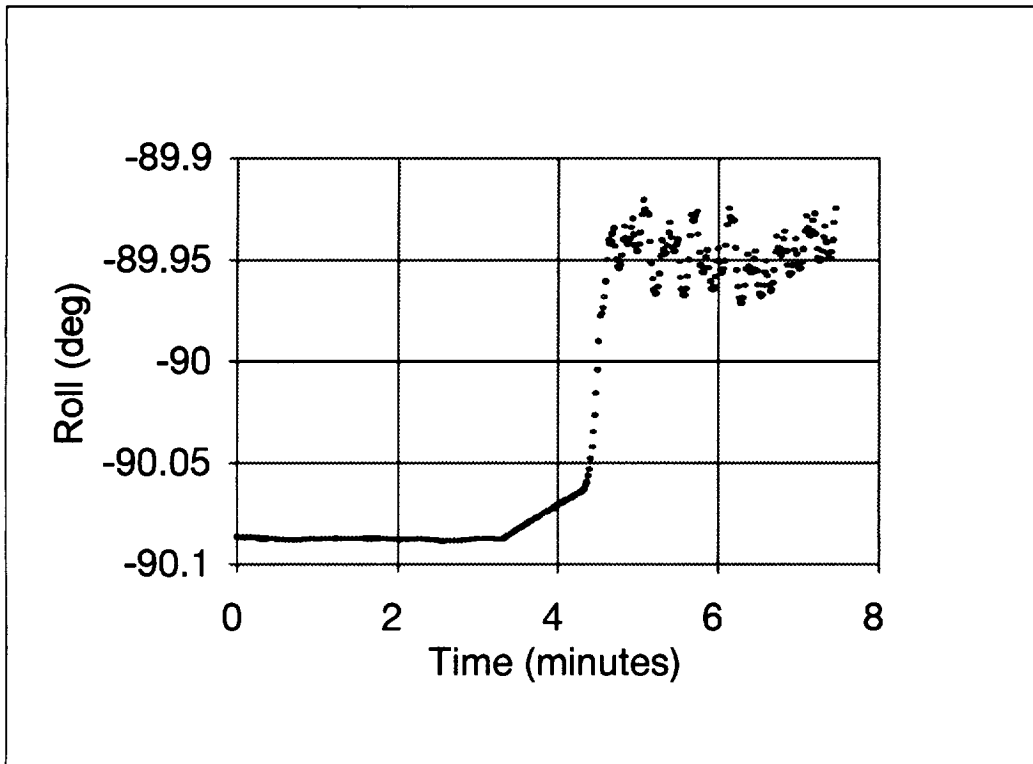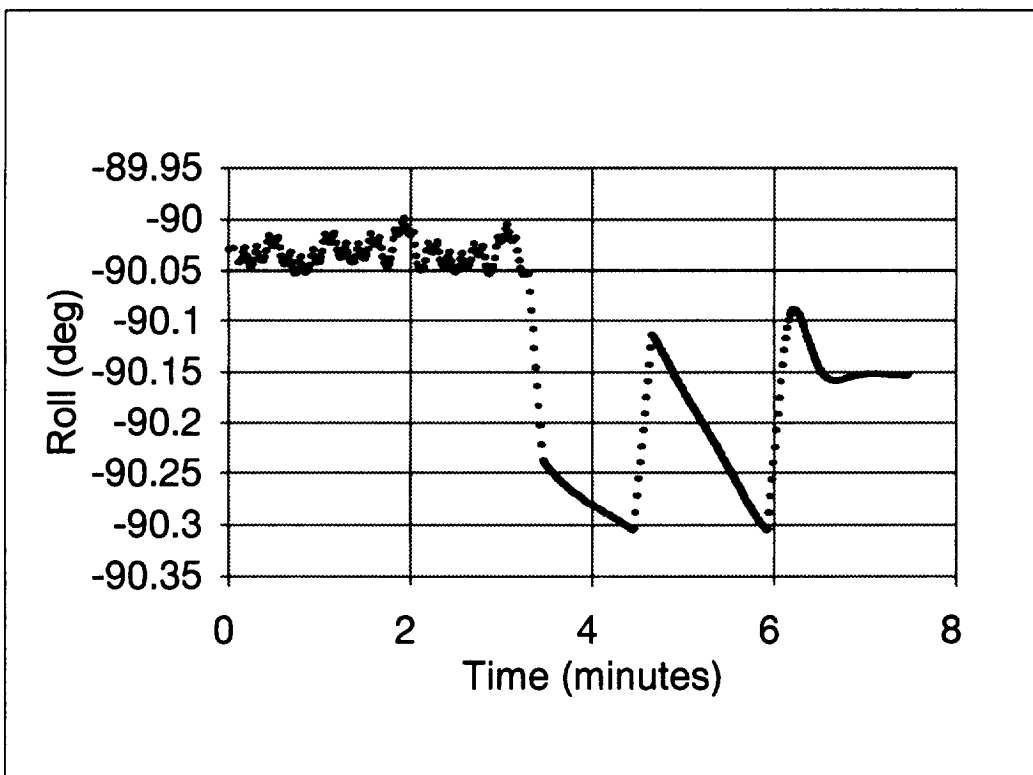
Figure 8. Roll Angle at Start of MCC2

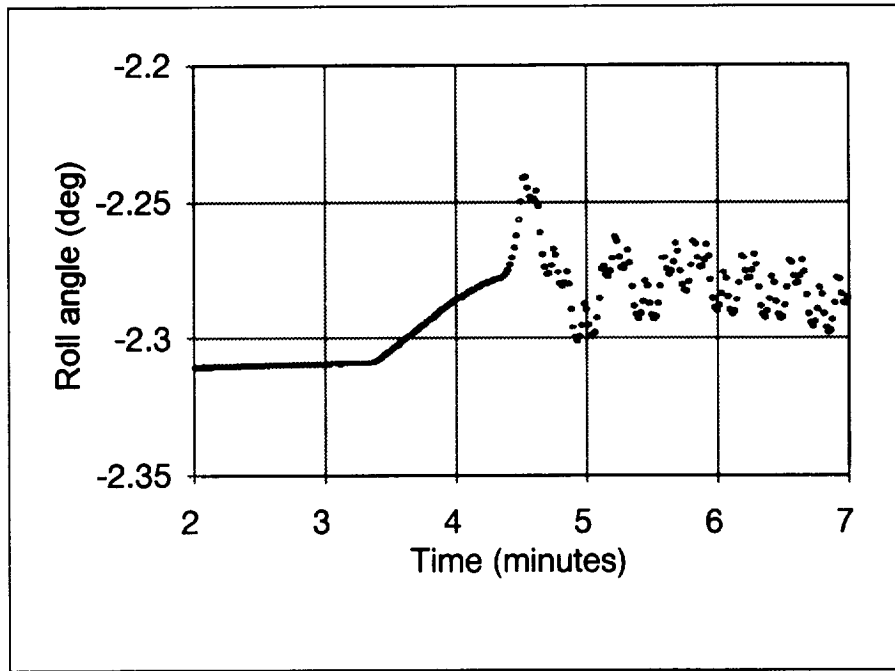Figure 9. Roll Angle at End of MCC2

119

Figure 10. Roll Angle at Start of HOI

The thruster model was evaluated from $\vec{T} = \vec{R} \times \vec{F}$ with CM at the beginning of transfer (BOT) value with solar panels deployed, yielding the following nominal torque matrix, Tmat, for thrusters 1A–8A (in Nm):

	1A	2A	3A	4A	5A	6A	7A	8A
Tx	0.0471	0.0848	0.0119	-0.0067	3.2634	-3.1015	-3.1512	3.1126
Ty	5.7332	-5.7727	0.3441	-0.2174	0.2971	0.3044	-0.3083	-0.2874
Tz	0.0616	-0.1494	-2.8434	2.8063	-0.0091	0.0001	0.0055	0.0119

For example, the –X orbit delta-V (case 1) uses thruster pair 1/2, with the Y (pitch) axis off modulated, yielding a nominal parasitic torque, T_{po}, computed from summing the torque vectors for the firing pair

$$\vec{T}_{po} = (0.1319 \quad -0.0395 \quad -0.0878)^T$$

The T_{po} components on the roll and yaw axes are compensated to conserve angular momentum. When the X (roll) axis control loop accumulates a pointing error in excess of the deadband, it induces a reactive torque from its on-modulated thruster pair (6/7 for +/- senses). Because $T_{po}(1)$ is positive, it must be compensated by the negative roll torque of magnitude 3.1015, leading to an expected value of 0.1319/3.1015 (or 4.2%) of the planned 900-second orbit delta-V burn, or 38-second split evenly between #6 and #7. Similarly, on the Z (yaw) axis, thruster pair 4/3 has an expected value of 0.0878/2.8063 (or 3.1%) of the main burn or 27.9 second with only thruster #4 activated. These values were verified by simulation. Because the on times grow linearly with the length of the orbit burn, they can be scaled for different burn times.

These predicted secondary firings were compared with telemetry during MCC1, and the results are shown in Table 3. When the burn times agreed to within a fraction of a percent, it confirmed that the maneuvers were proceeding nominally.

120

The initial thruster alignment was so accurate that no recalibration was needed; however, we had prepared a technique to assist in thruster realignment if necessary. While the nominal T_{po} is a predictor of off-axis firings, the observed firing times from telemetry can be used to infer actual thrust torque values and alignment. A sensitivity study was performed in advance to prepare for possible nonnominal conditions and to establish a baseline for their resolution, using prelaunch values for the nominal thruster model. Nominal and perturbed thruster parameters, efficiency, and CM were used to create the sensitivity matrix. These results were available to aid in matching observed thruster firing times. Because the problem is underdetermined, the most sensitive parameters were considered first.

Table 3. Predicted and Observed Thruster Firing Times From X-1 Maneuver

Thruster Number	Predicted On Time	Observed On Time
1A	900 sec (nominal)	903.9111
2A	900 sec	896.0319
3A	0	0.0
4A	28	27.2743
5A	0	0.0
6A	19	20.5540
7A	19	20.5540
8A	0	0.0

3.2.2 Postmaneuver Thruster Analysis

After several maneuvers, the secondary firings began to be predicted less well, and we adjusted the SOHO thruster model using the principle of conservation of angular momentum. As discussed above, in CSP mode the momentum wheels are free running and the attitude axes are controlled to zero; thus, each maneuver segment must conserve total angular momentum. The burn times of the primary and secondary thrusters were evaluated for MCC1 and MCC2 maneuver segments based on the change in angular momentum, $d\vec{L}$ ($- \vec{T}$*dt), calculated from the thrust torque model and the actual burn times. Any residual dL above the noise level indicates inaccuracy in the thruster model.

The technique of plant identification was used to improve the salient parameters in the model and minimize the error vector dL, and the validity of the resultant model was tested by application to the next maneuver (HOI). In control theory, plant identification is the term applied to the systematic process of estimating the parameters that control the dynamics of the system under study, in our case the SOHO ACS under thrusting. The process diagram is presented in Figure 11. Although it could be completely automated when necessary, in the present case it was implemented as a computer-assisted procedure with the analyst in the loop. The process was facilitated by use of models already available for the thruster torque, sensitivity partials, and a CM model as a linear function of fuel use between the BOT and BOL phases.

The procedure for computing the nominal angular momentum change for each maneuver segment is as follows:

- Compute the maneuver dL error vector using nominal values for the thruster/CM model, with the root-sum-squared (RSS) dL error vector as a figure of merit.

- Balance the efficiency of the primary thrusters to minimize their error along the primary axis.

- Adjust other torque model parameters in the order of their sensitivity to minimize the sum of all maneuver error vectors.

121

Torque is modeled from $\vec{T} = \vec{R} \times \vec{F}$ with current values of CM and efficiency, and the change in angular momentum $d\vec{L}$ ($= \vec{T}$ *dt) is calculated from

$$d\vec{L} = T_{mat} * \vec{t}_{on_i}$$

where T_{mat} is the 3×8 matrix of torques for the eight thrusters, adjusted for CM motion, and $\vec{t}_{on_i}$ is the 8×1 vector of thruster on times for the ith maneuver. The RSS is given by

$$RSS_i = \sqrt{(dL_1)^2 + (dL_2)^2 + (dL_3)^2}$$

and the overall figure of merit to be minimized is given by
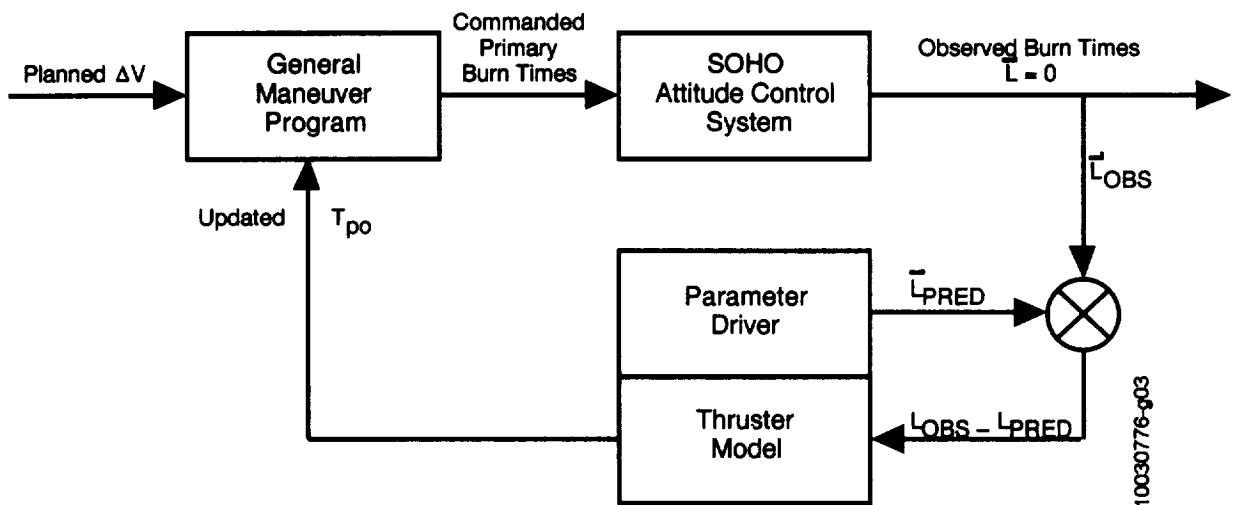
$$RSS_{tot} = \sum_i RSS_i$$

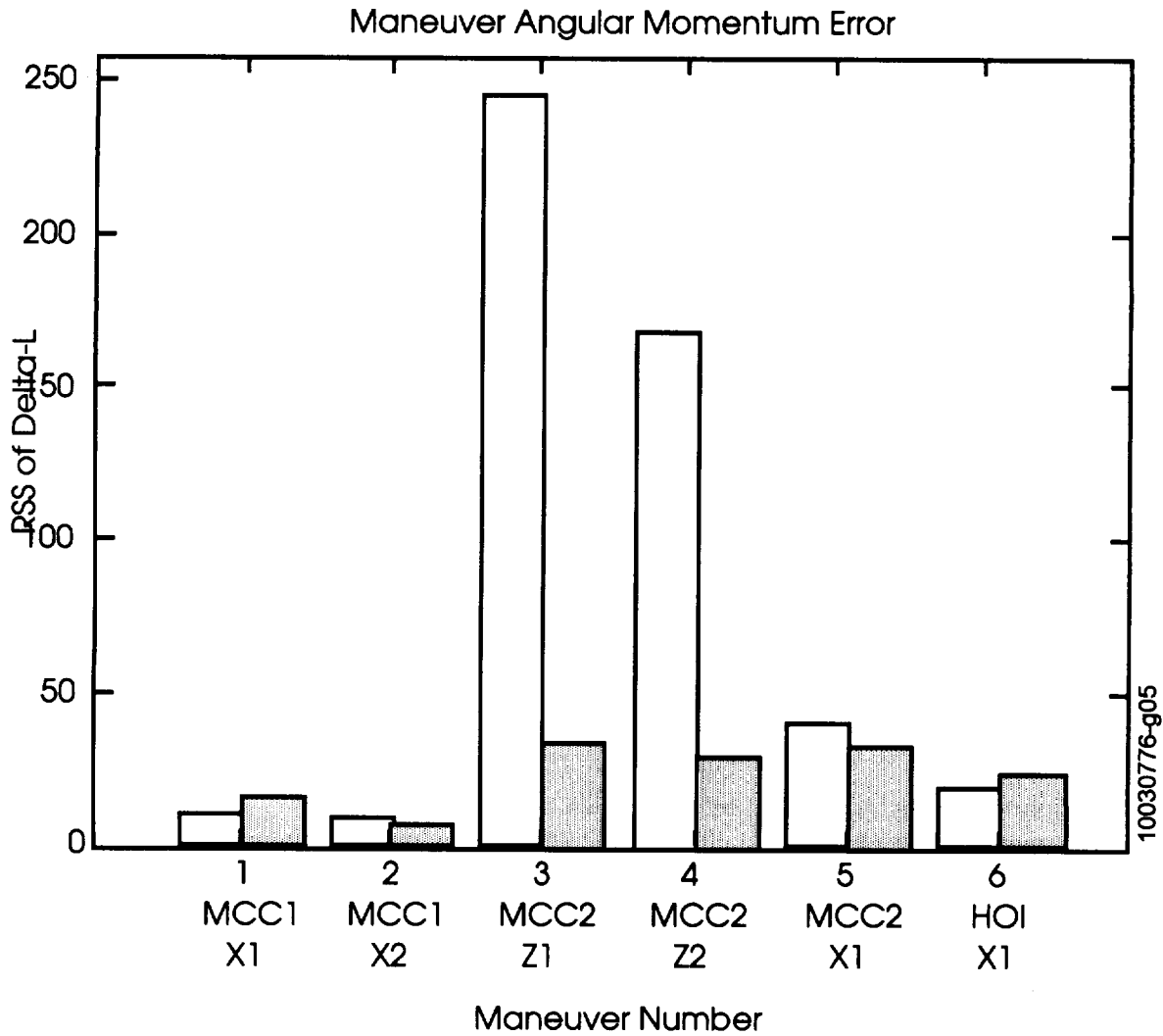**Figure 11. Schematic Diagram of Plant Identification**

3.2.3 Thruster Results

The results of thruster model tuning for MCC1 and MCC2 are shown in Figure 12. The initial model (unshaded) fit the –X delta-V maneuvers well, but the Z delta-V maneuvers fit poorly; sensitivity analysis showed that these were strongly affected by the exact model of CM, both the initial value (bias) and the motion (slope) with fuel usage.

The results of the plant identification are as follows:

Efficiency correction to thruster 8:	dEff(8) = –0.0148
Variation in the initial CM:	dcm = (0.0047, 0.0, 0.001)
Variation in slope of CM function:	dcm0 = 0.99

The shaded bars show a reduction in maneuver errors of about a factor of 5 with the new values in the thruster model.

Figure 12. Maneuver Angular Momentum Error

4.0 Conclusions

The conclusions from this study are as follows:

- The use of feed-forward torques is effective in reducing attitude hangoff in flight.

- Simulation is a valuable tool for understanding the operation of onboard attitude control systems and preparing operational procedures.

- Attitude effects can provide valuable diagnostic information on the thrusters in addition to that available from telemetry and postmaneuver orbit determination.

- COTS tools such as MATLAB® provide means for rapid implementation of computer-assisted analysis.

References

1. British Aerospace Ltd., Sh-BAe-RP-1321, Issue 3, Performance Review Document, Volume V: *Coarse Sun Pointing Mode*, J. Smallwood, September 1993

2. Goddard Space Flight Center, Flight Dynamics Division, 533-FDD-93/088R0UD0, *Disturbance Torque Estimates for the SOHO Mission*, T. Becher (CSC) and J. Rowe (CSC), prepared by Computer Sciences Corporation, September 1993

3. British Aerospace Ltd., SH-BAe-RP-1317, Issue 2, Performance Review Document, Volume I: *Mathematical Models*, P. Singh, July 1993

4. – – –, SH-BAe-RP-1324, Issue 2, Performance Review Document, Volume VIII: *Additional Analyses*, D. F. Lebrun, J. Smallwood, T. D. Wood, February 1994

5. – – –, SH-BAe-RS-632, Issue 8, *SOHO ACS Software User Requirements*, T. J. Biglin, March 1994